Optoelectronic properties of thin film $Cu_2ZnGeSe_4$ solar cells

S. Sahayaraj[1,2,4] G. Brammertz[1,2], B. Vermang[3,4], T. Schnabel[7], E. Ahlswede[7], Z. Huang[1,2,4], S. Ranjbar[1,2,6], M. Meuris[1,2], J. Vleugels[8] and J. Poortmans[3,4]

[1] imec division IMOMEC - partner in Solliance, Wetenschapspark 1, 3590 Diepenbeek, Belgium.
[2] Institute for Material Research (IMO) Hasselt University – partner in Solliance, Wetenschapspark 1, 3590 Diepenbeek, Belgium.
[3] imec –partner in Solliance, Kapeldreef 75, 3001 Leuven, Belgium.
[4] KU Leuven, Department of Electrical Engineering, Kasteelpark Arenberg 10, 3001 Heverlee, Belgium.
[5] Laboratory for photovoltaics, University of Luxembourg, rue du Brill 41, 4422 Belvaux, Luxembourg
[6] I3N - Departamento de Física, Universidade de Aveiro, Campus Universitário de Santiago, 3810-193 Aveiro, Portugal.
[7] Zentrum für Sonnenenergie- und Wasserstoff- Forschung Baden-Württemberg, 70565 Stuttgart, Germany
[8] KU Leuven, Department of Materials Engineering, Kasteelpark Arenberg 44, 3001 Heverlee, Belgium

Abstract: The fabrication and properties of a Ge-based Kesterite $Cu_2ZnGeSe_4$ (CZGSe)solar cell are discussed**.** The existence of the quaternary compound has been verified by physical methods such as X Ray Diffraction (XRD) and Energy Dispersive Spectroscopy (EDS). The $Cu_2ZnGeSe_4$ solar cell has a power conversion efficiency (PCE) of 5.5% under AM1.5G illumination which is among the highest reported for pure Ge substitution. Detailed low temperature current-voltage and time-resolved photoluminescence measurements show that the $Cu_2ZnGeSe_4$ absorber has less bulk defects and less band tailing in contrast to the typical characteristics of $Cu_2ZnSnSe_4$ devices. These beneficial opto-electronic properties also resulted in a high open circuit voltage (V_{oc}) of 744 mV which is amongst the highest values reported for Kesterite materials.

1. Introduction:

Detailed calculations [1] and simulations [2] revealed that the largest individual energy loss factors in solar cells with a single absorber material are due to carrier thermalization, which can be minimized with a tandem cell geometry, i.e. a sandwich of a low band gap (E_{gap}) bottom cell (like Si or Cu (In,Ga)Se_2 (CIGS)) with $E_{gap} \sim 1.1$ eV) and a high band gap top cell with $E_{gap} \geq 1.4$eV. Kesterite materials are a potential candidate for the top cell due to their tunable direct band gap (1 eV – 3.1 eV) [3] through cation and anion substitution along with their CIGS-like excellent optical properties. Increasing the band gap by using the pure sulfide version is a readily available option. The maximum efficiency obtained with sulfide Kesterites is not beyond 9%. Possible reasons for this are discussed in [4]. Higher efficiencies have been possible with a mixture of both S and Se but this results in low band gaps. A few authors have reported that Ge incorporation in Kesterites along with Sn results in improved efficiencies , improved grain morphologies, increased minority carrier lifetimes and lower V_{oc} deficits [5-8]. However, the band gap achieved in all the cases listed above is around 1.2 eV which is not suitable for tandem cell geometries. Band gaps higher than 1.2 eV can be achieved by pure Ge substitution instead of a mixture of Sn and Ge. Except for the work done by Schnabel et al.,[9] no other group has reported significant efficiencies with pure Ge substitution. In their work Schnabel et al., reported a maximum conversion efficiency of 5.1% for a solution based $Cu_2ZnGeS_xSe_{4-x}$ solar cell with a band gap of 1.5 eV. In this work, a similar approach of replacing Sn completely by Ge in the Kesterite is presented, resulting in an absorber material

with a band gap of 1.4 eV. A solar cell with a maximum PCE of 5.5 % and an unprecedented open circuit voltage (V_{oc}) of 744 mV has been obtained.

2. Experiments and Methods

2.1) Sample Fabrication

All solar cells were fabricated on a 3 mm thick, 25 cm^2 soda lime glass substrate covered by 400 nm of Molybdenum (Mo) as electrical back contact. The sheet resistance of Mo is 0.1Ω/sq. The constituent elements that make up the absorber layer are deposited in a Cu (170)/Zn(125)/Ge(180) sequence on top of the Mo-coated glass by means of electron beam evaporation. The numbers in brackets indicate the thickness of the metals in Nano meters. The precursor films were selenized at elevated temperatures (470ºC) in a custom made "Halogen furnace". The tri layer was held in a square shaped graphite box with provision to place Se pellets on the sides of the box. The annealing is carried out in a Se-rich atmosphere created by 1 g of Se in the graphite box to form crystalline CZGSe thin films. The duration of the entire annealing cycle (ramp , dwell and cooling) is 3 hours where the dwell time is 10 minutes. The temperature was measured from thermocouples connected to the outer edges of the graphite box which is in contact with the sample. Therefore the temperature on the surface of the sample can be higher than 470ºC. The selenised absorbers were then immersed in a 3 wt.% aqueous KCN solution for 90 s to remove secondary phases, elemental selenium and native oxides from the absorber surface. To obtain functional solar cells, a 50 nm thick CdS layer is deposited via chemical bath deposition followed by an intrinsic ZnO (80 nm) and an aluminum-doped ZnO (400 nm) layer by sputtering followed by the deposition of 50 nm of Ni and 1 µm thick Al fingers as front contact.. Individual cells with an area of approximately 0.5 cm^2 were laterally isolated by mechanical scribing.

2.2) Physical Analysis.

The surface morphology and chemical composition of the CZGSe thin films were evaluated by a scanning electron microscope (SEM, Nova 200, FEI), equipped with an energy dispersive X-ray analysis (EDX) system. The accelerating voltage used for the EDX analysis was 20 kV. X-ray diffraction (XRD) measurements were carried out on a X'Pert Pro MRD X-ray diffractometer in the conventional Bragg-Brentano ω-2θ geometry using Cu K_α (1.5411 A˚) radiation as incident beam.

2.3) Electrical and Optical Analysis.

The processed solar cells were analyzed using Current-Voltage (IV) measurements, using a 2401 Keithley Source meter, under standard test conditions for Kesterite solar cells with a solar simulator system using an AM1.5G spectrum with an illumination density of 1000 W/m^2 at 25°C. The external quantum efficiency (EQE) has been measured at room temperature using a laboratory-built system with a grating monochromator-based dual-beam setup under chopped light from a Xe lamp. The doping profile of the absorbers was measured by capacitance voltage (CV) measurements, which were performed with an Agilent 4980A LCR-meter with frequencies varying from 1 kHz to 1 MHz. The excitation dependent photoluminescence

analysis was measured using a Hamamatsu C12132 near infrared compact fluorescence lifetime measurement system equipped with a cryostat that can be cooled down to liquid N_2 (77K) temperatures. The tool uses 15 kHz, 1.2 ns pulsed 532 nm laser and the average laser power was varied between 1 mW to 56 mW to illuminate an area of 3 mm diameter on the measured solar cell.

3. Results and discussion

3.1) Physical properties of the Absorber

Fig 1a shows the surface morphology of the KCN-etched CZGSe absorber made up of densely packed micrometer sized grains. The composition of the CZGSe thin film absorber layer was deduced from SEM - EDX measurements. The thin film layer was found to be Cu-poor and Zn-rich with [Cu]/[Zn]+[Ge] and [Zn]/[Ge] ratios of 0.78 and 1.18, respectively. The cross section view of the entire CZGSe solar cell is provided in Fig.1b). From the cross SEM image, the average absorber thickness was found to be 1.2 µm. Although it is not very easy to specify the exact thickness of the $MoSe_2$ phase, a thin layer of possibly 60 nm is present at the interface of CZGSe/Mo. Along with the big sized CZGSe grains, very small and bright particles are also seen. The crystalline phases in the XRD pattern shown in Fig 1c) were matched by PDF cards from the ICDD–PDF 4 database [10] and confirmed the formation of Ge substituted Kesterite. Besides CZGSe, a small amount of ZnSe is also present due to a high Zn/Ge ratio along with $MoSe_2$. Since the XRD measurement was performed on the solar cell ZnO peaks are also present. Combining the information from cross section SEM and XRD it can be concluded that the small bright particles observed in fig.1b) along with CZGSe belong to the ZnSe secondary phase. The minority carrier lifetime was measured at room temperature from time resolved photoluminescence (TRPL) measurements is shown in Fig 1d) along with the photoluminescence (PL) peak Fig.1e) shown as an inset of Fig 1d) reveals a band gap of 1.4 eV . Density functional theory (DFT) calculations [11] on the optical properties of $Cu_2ZnGeSe_4$ show that the absorber has a direct band gap and substitution of Ge in the place of Sn in Kesterite CZTS structure only changes the position of the conduction band minimum resulting in a higher band gap. Therefore it is very likely that the PL measurement in this case reveals the direct band gap of the quaternary absorber. A three exponential fit to the photoluminescence decay curve was established. The three components of the fit have lifetimes of respectively 0.1ns, 1.3 ns and 12 ns, respectively. At present it is not quite clear which of these components corresponds to the minority carrier lifetime. Further measurements of the decay time at 77 K, shown later in Fig 4d , seem to indicate that at least the longest component of the decay is related to some sort of particle trapping, not being related to the minority carrier lifetime.

Optoelectronic properties of thin film $Cu_2ZnGeSe_4$ solar cells

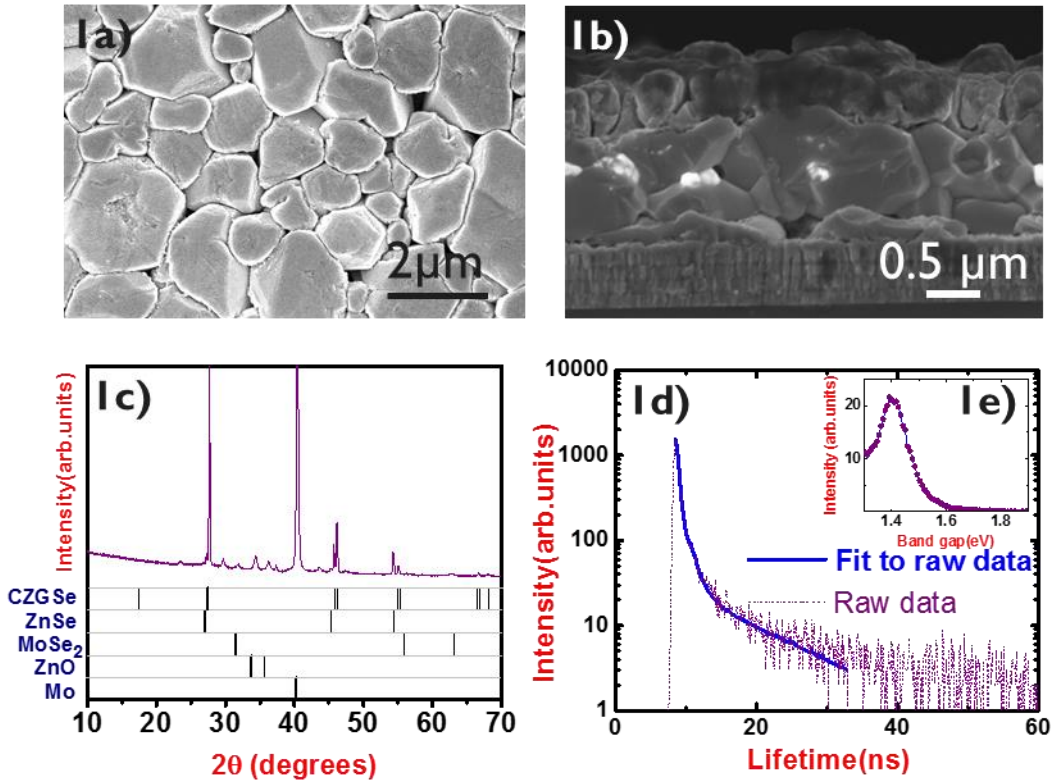

Figure 1a) & 1b) X-SEM images of the CZGSe thin film absorber and CZGSe thin film solar cell. Figure 1c) XRD pattern of the CZGSe thin film solar cell. Figure 1d) Time resolved photoluminescence measurement showing the band gap and Figure 1e) (shown as an inset) Photoluminescence spectrum of CZGSe absorber.

3.2) Detailed electrical and optical properties.

The final device has 6 functional cells and the average efficiency of the device was (4.5 ± 1) %. The best cell from the sample is presented in Fig 2a). Although the solar cell has an impressive V_{oc}, it's efficiency is limited by a low fill factor (FF) of 46% and a low short circuit current density (J_{sc}) of 16 mA/cm^2. The reason for these low values is most likely due to the high series resistance (R_s) equal to 14 Ohm cm^2 in the circuit. The origin of the R_s is uncertain. It could arise due to the presence of secondary phases (ZnSe, $MoSe_2$) or due to a barrier at the heterojunction interface or the backside interface. The shunt resistance of the device under illumination is 670Ω.cm^2 which seems to be a reasonable value and leakage currents are not seen from the dark curve. The poor FF is not really due to the shunt resistance. It seems quite clear though that the large series resistance value is a large factor limiting the power conversion efficiency of the device, so further investigations should find the root cause of this resistance. The p- type doping of the absorber measured by CV profiling at 54kHz fig.2b) is of the order of 10^{15} /cm^3, a value similar to our best $Cu_2ZnSnSe_4$ (CZTSe) devices [12,13]. The optical losses of the solar cell were studied by External Quantum Efficiency (EQE) measurements shown in Fig 2c). The EQE spectrum reveals significant collection losses due to parasitic absorption by TCO's and incomplete absorption by CdS up to 540 nm. The collection efficiency in the infra-red region is also low and it keeps dropping indicating reduced collection

of carriers created deep in the absorber. The maximum EQE at 550 nm does not reach close to unity. This region corresponds to the vicinity of CdS/ CZGSe interface. The fact that not all photons contribute to the J_{sc} could be due to a band alignment issue which might be unfavorable for carrier collection. These findings suggest that there is some problem still in the solar cell in collecting all the charge carriers even at zero bias.

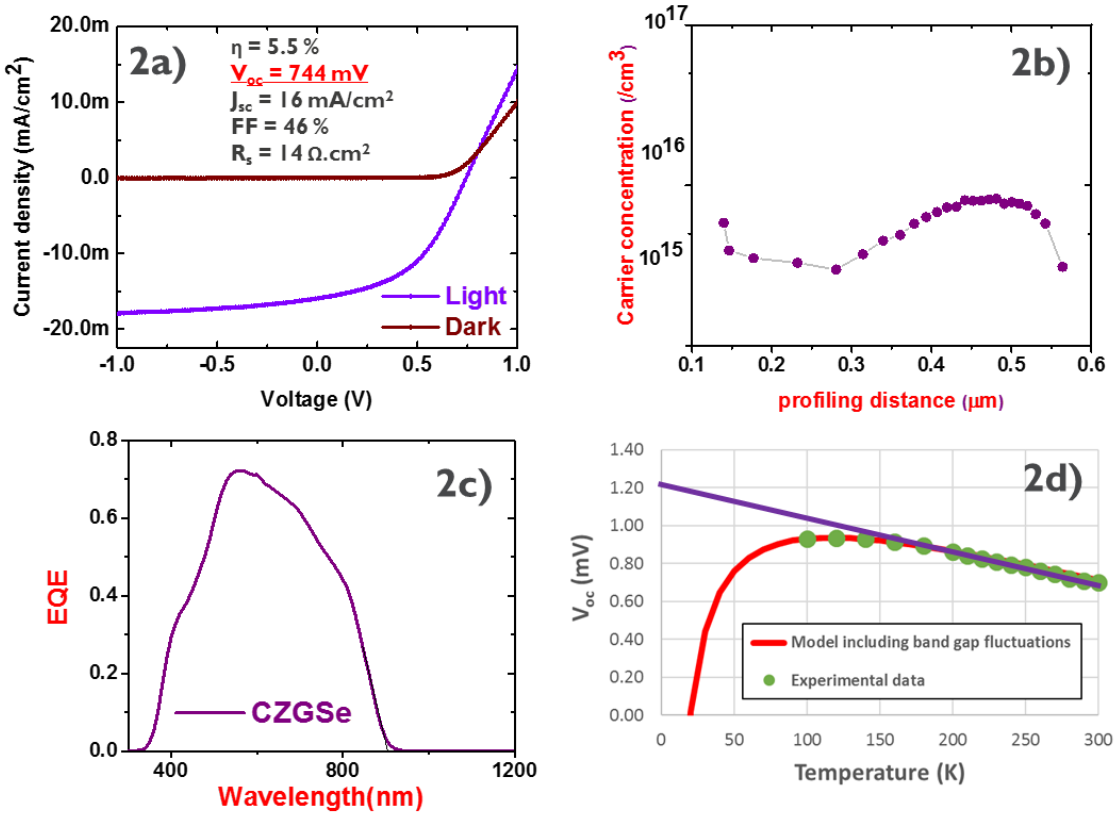

Figure 2a) Illuminated AM 1.5G and Dark IV curves along with solar cell parameters. Figure 2b) Capacitance – voltage profiling showing the doping density of the CZGSe solar cell Figure 2c) External quantum efficiency measurements of the CZGSe solar cell Figure 2d) Temperature dependent IV measurements involving model for band gap fluctuations of CZGSe solar cell.

To understand further the semiconductor nature of the absorber, IV and PL measurements were performed at 77K. The behavior of V_{oc} with temperature is shown in Fig 2d.The extrapolation of the V_{oc} at 0K usually is interpreted as giving the activation energy of the dominant recombination process in the solar cell [14]. It can be seen that the extrapolated V_{oc} at 0K is 1.22 V, a value lower than that of E_g/q (1.4V) which is an indication that the V_{oc} is limited by recombination at the absorber – buffer interface similar to most Sn based Kesterites. An alternative interpretation to the data shown in Fig. 2d) could be given by fitting the data with the equation derived by Rau et al, shown below in the case of an absorber presenting lateral band gap fluctuations [15].

$$V_{OC} = \frac{\overline{E_g}}{q} - \frac{\sigma_{E_g}^2}{2kTq} - \frac{kT}{q}\log\left(\frac{J_{00}}{J_{SC}}\right)$$

As can be seen in figure 2d, a good fit to the experimental data can be obtained using as fitting parameters, the activation energy of the dominant recombination process equal to the band gap value 1.4 eV and a magnitude of the band gap fluctuations of 65 meV. Figure 2d could also be interpreted in a way that the dominant recombination process is in the bulk of the absorber and not at the interface and that the intersect with zero Kelvin is reduced because of the presence of a relatively large amount of band gap fluctuations in the absorber.

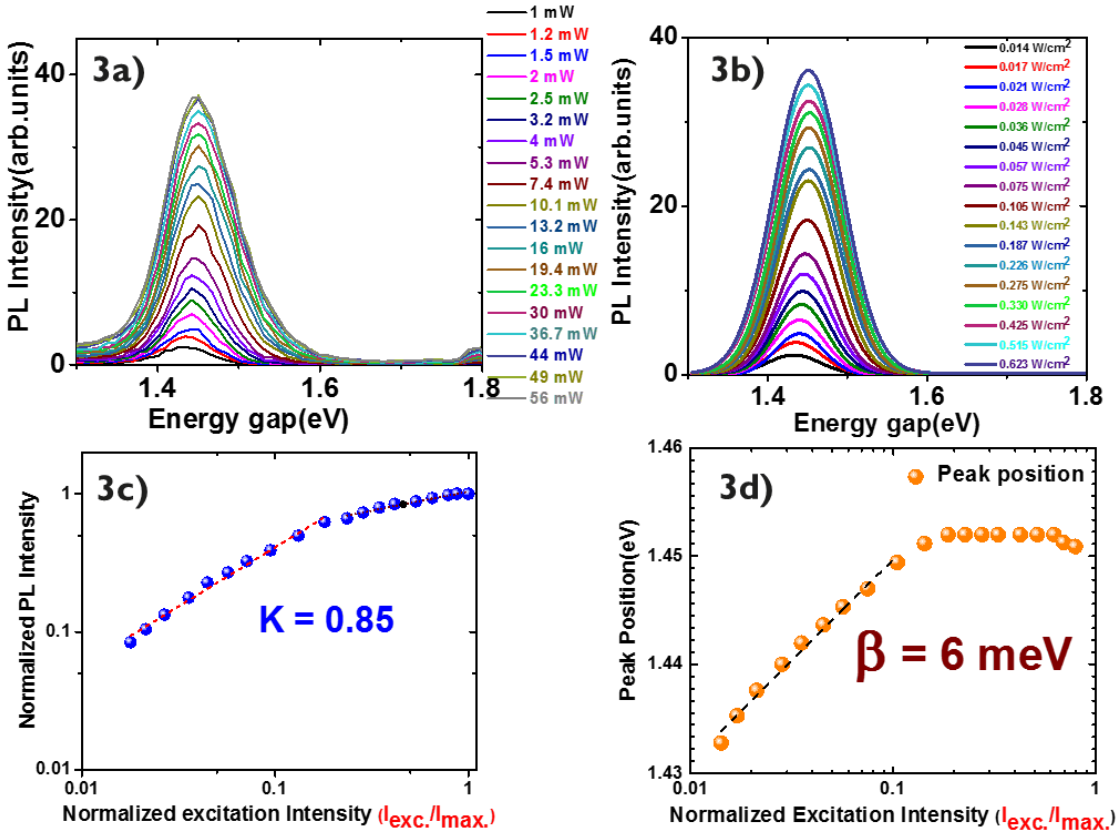

Figure 3a) Raw data of the PL spectrum of CZGSe solar cell as a function of the laser excitation Intensity. Figure 3b) Fitted data of the PL spectrum of the CZGSe solar cell peak fitting. Figures 3c) and 3d) Plots to determine the k exponent and rate of blue shift with increasing excitation in CZGSe solar cell.

The PL emission spectrum of the absorber as a function of the laser excitation intensity at 77K is shown in Fig.3a). Fig.3b) shows the detailed Gaussian peak fitting of the raw data which reveals only one emission for all the excitation intensities used. The peak positions vary from 1.43 eV for the lowest excitation intensity (0.014W/cm^2) and blue shift up to 1.45 eV with increasing excitation intensity (up to 0.143 W/cm^2) and saturate. Beyond this point, only at very high excitations the peak centers were found to red shift slightly. This behavior of the

emission spectrum is in line with a CZTS device [16] where the transitions are classified under the Quasi Donor to Acceptor (Q-DAP) Model. The assessment of the peak signatures was performed by plotting the normalized excitation intensity against the observed PL Intensity Fig.3c) based on the observation that the luminescence yield of a transition generally obeys the expression $\mathbf{I_{exc}} \alpha \mathbf{I_{PL}^k}$ [17,18]. From this plot it can be seen that the k exponent is below 1 which is characteristic for defect related recombination in the absorber [19] adding further support to the Q-DAP model. Next to the energy dependence of the PL peak, the excitation intensity was analyzed. From literature this dependence is explained by the expression $E = \beta \ln(I/I_{max})$[20,21] where E is the energy of the PL peak, I is the intensity of the PL peak and β is the energy shift in the peak position. From the analysis of the experimental data in Fig 3d) in the linear region, β was calculated to be 6 meV. A small blue shift of the peak position at a rate of 1–2 meV/decade with increasing excitation power is a characteristic of classical Donor to Acceptor (DAP) emission [22,23]. In the case of DAP recombination when the excitation intensity increases, the concentration of occupied donors and acceptors also increase thereby reducing the average distance between these defects which gives rise to a higher Coulomb interaction energy resulting in a blue shift described by the equation.

$$\mathbf{E_{DA} = E_g - E_A - E_D + E_{Coul} \ \ where \ \ E_{Coul} = e^2/4\pi\varepsilon_0\varepsilon_r r} \qquad \mathbf{(1)}$$

where E_g is the energy gap , E_D and E_A are the donor and acceptor ionization energies, respectively, e is the electron charge and ε_0 is the permittivity of free space, ε_r is the static dielectric constant and r is the distance between the donor and acceptor states.

A blue shift at the rate of 6 meV/ decade is difficult to achieve with classical DAP recombination, in which case the blue shift is only due to pairs recombining over smaller and smaller distances with increasing laser excitation. The origin of these high values is probably related with band gap or electrostatic potential fluctuations in the absorber , a problem native to Kesterite devices. With the band gap fluctuations being quantified by low temperature IV measurements it looks alright to conclude that optical transitions in CZGSe follow the Q- DAP model. A useful feature of the Q – DAP model is that the saturation of the blue-shift in the PL peak can be used to calculate the spacing between these defects by equating the magnitude of the blue-shift with the Coulombic term in Eq. (1) [16]. Using a value of 6.7 for the relative permittivity of CZGSe, a defect spacing of 10 nm , a Q-DAP density of $2.4 \times 10^{17}/cm^3$ {under the assumption $r = (3/4\pi N_d)^{1/3}$}[24] was calculated. This value is 1 - 2 orders of magnitude lower than the defect densities of CZTS[16] and CZTSe [25] devices.

The minority carrier lifetime measurements of CZGSe show a significant difference from CZTSe. In order to explain this difference, a CZTSe device with a power conversion efficiency of 8.6% (without Anti Reflection Coating) similar to the one described in [12] fabricated in imec has been compared with the CZGSe solar cell in discussion. At room temperatures the lifetimes of CZGSe Fig.1d) and CZTSe Fig. 4a) are similar reaching values up to several nanoseconds. However, at 77K the lifetime of CZTSe increases by several orders of magnitude reaching values up to a few µs. Fig.4b). The position of the PL peak Fig.4b) is also found to red shift dramatically below the band gap. The reason behind this behavior can be understood when electrostatic potential fluctuations are invoked. In the case of electrostatic potential

fluctuations, electrons and holes are spatially separated and any recombination process requires the tunneling of carriers. Moreover because of insufficient thermal energy at reduced temperatures, these electron and holes cannot jump over the fluctuations and therefore become localized in these wells [26]. The electrons and holes separated by short distances rapidly recombine. However, the majority of the carriers are separated by high barriers at larger distances and therefore the recombination time becomes large [27] in CZTSe. One obvious consequence of the electrostatic potential fluctuations is the formation of band tail states below the true band-gap energy of the CZT(S,Se) absorber identical to what was observed in imec CZTSe device as well. The extent of this band tailing can be quantified from the Γ parameter that can be deduced from Low temperature PL analysis and gives the average depth of these potential fluctuations in the absorber from the formula given in [24]. The calculation yields values of 30 meV and 18 meV for CZTSe and CZGSe respectively. The formation of band tails can also result from band-gap fluctuations. It is clear that bandgap and electrostatic potential fluctuations are fundamentally different on the microscopic scale. In the case of band-gap fluctuations, electrons and holes are not in general spatially separated and therefore enhanced lifetimes at low temperatures are not expected [27]. This is exactly the situation observed in the CZGSe absorber. The minority carrier lifetime drops to below 1 ns and it also remains independent of the excitation intensity as it can be seen from Fig.4d) for different PL excitation intensities shown in Fig.4c), a behavior diametrically opposite to that of CZTSe devices at cryogenic temperatures. The low-temperature TRPL data therefore suggest that a dominant contribution to the observed band tailing in CZT(S,Se) samples comes from the electrostatic potential fluctuations which is totally absent in the CZGSe absorber. However, at room temperatures defects responsible for recombination that were frozen at cryogenic temperatures could become active and might act as carrier trap states. This would give rise to recombination that results from carrier de - trapping by defect states to the bands resulting in longer decay times characterized by longer tails as seen in Fig. 1d) of the TRPL spectrum. It is possible in CZGSe that at room temperature the carrier lifetime is totally influenced by defects and the real minority carrier lifetime of CZGSe absorber is a value less than a nanosecond. Besides several reasons explained earlier the low minority carrier lifetime could also play a part in the poor carrier collection efficiency of the solar cell which was witnessed from EQE measurements shown in Fig.2c).

Optoelectronic properties of thin film $Cu_2ZnGeSe_4$ solar cells

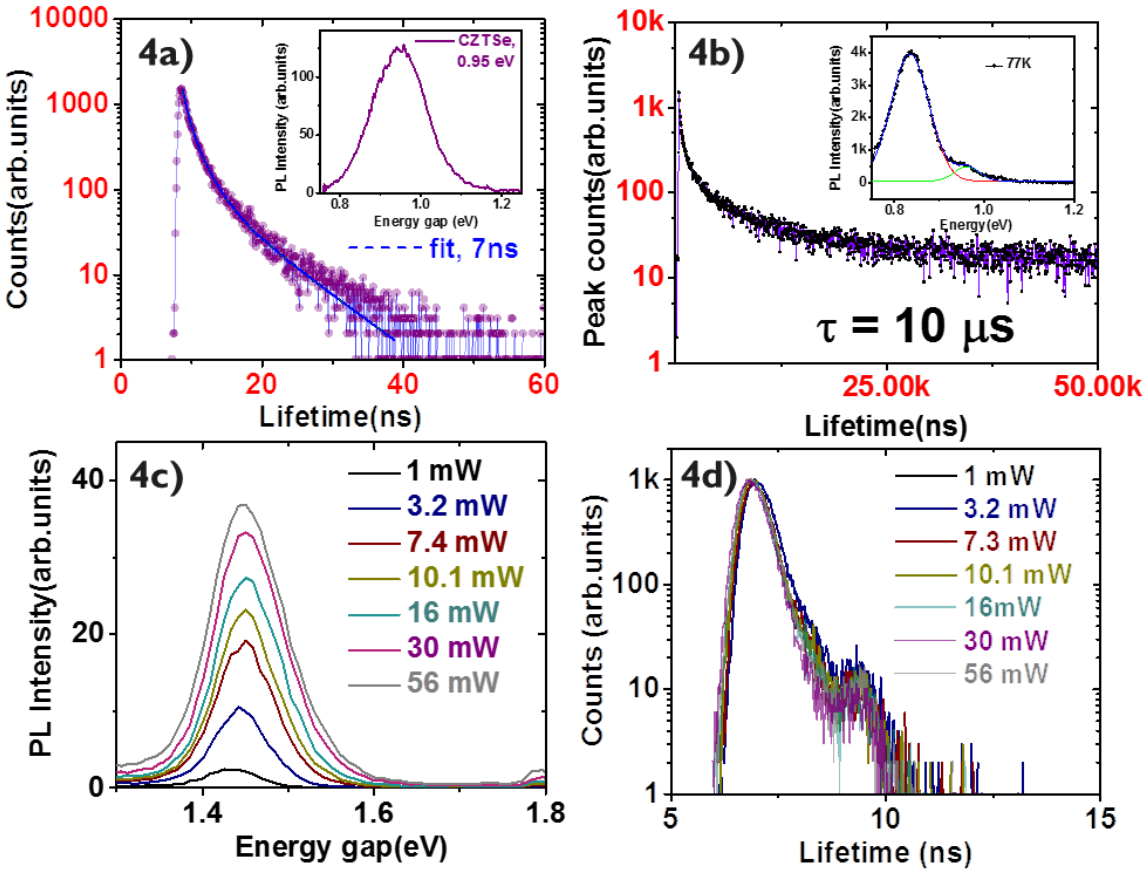

Figure 4a) Minority carrier lifetime of a 8.6% CZTSe device and its photoluminescence curve (shown as inset) at room temperature. Figure 4b) Minority carrier lifetime of 8.6% CZTSe device and its photoluminescence curve (shown as inset) at room temperature. Figure 4c) Photoluminescence spectrum of CZGSe measured at different laser excitation intensities. Figure 4d) Minority carrier lifetime of 5.5% CZGSe device measured at different laser excitation intensities for CZGSe solar cell at 77K

Summary:

A Ge based Kesterite solar cell has been fabricated. Detailed investigation on the electrical and optical properties show that the p type absorber does suffer less electrical losses from band tailing, a property quite distinct for CZTSe, resulting in a particularly large Voc of 744 mV. The main efficiency limiting factors are the low fill factor (46%) and J_{sc} (16 mA/cm^2) which can be linked to a high series resistance R_s of 14 Ohm cm^2 and a relatively low minority carrier lifetime of the order of 1 ns, leading to imperfect current collection. Mainly the reduction of the large series resistance could lead to further big improvements in the conversion efficiency, making $Cu_2ZnGeSe_4$ a promising absorber material for thin film solar cell applications.

Acknowledgements:

This research is partially funded by the Flemish government, Department Economy, Science and innovation. This research has received funding from the European Union's Horizon 2020 research and innovation program under grant agreement No 640868.

Optoelectronic properties of thin film $Cu_2ZnGeSe_4$ solar cells

References:

[1] A. Polman, H.A. Atwater, "Photonic design principles for ultrahigh-efficiency Photovoltaics", Nat. Mater. 11 (2012) 174–177.

[2] T. P. White, N. N. Lal, and K. R. Catchpole, Tandem Solar Cells Based on High-Efficiency c-Si Bottom Cells: Top Cell Requirements for >30% Efficiency, IEEE Journal of Photovoltaics 4, (2014), 208-214.

[3] D.B Khadka, J. Kim, "Band Gap Engineering of Alloyed $Cu_2ZnGe_xSn_{1-x}Q_4$ (Q=S,Se) Films for Solar Cell", J. Phys. Chem. C 119, (**2015)**,1706,

[4] T. Gershon, Y.S. Lee, R. Mankad, O. Gunawan, T. Gokmen, D.Bishop, B. McCandless, and S. Guha. "The impact of sodium on the sub-bandgap states in CZTSe and CZTS". Appl. Phys. Lett. 106, 123905 (2015)

[5] S. Kim, K. M. Kim, H. Tampo, H. Shibata, K. Matsubara and S. Niki, Ge-incorporated $Cu_2ZnSnSe_4$ thin-film solar cells with efficiency greater than 10%" Sol. Energy Mater. Sol. Cells, 144, (2016), 488–492

[6] S. Kim, K.M. Kim, H. Tampo, H. Shibata, and S. Niki, "Improvement of voltage deficit of Ge-incorporated kesterite solar cell with 12.3% conversion efficiency", App. Phy. Express 9, (2016),102301.

[7] A.D. Collord and H.W. Hill house "Germanium Alloyed Kesterite Solar Cells with Low Voltage Deficits" Chem. Mater.7, (2016), 2067–2073.

[8] C.J. Hages, S. Levcenco, C.K. Miskin, J.H. Alsmeier, D.A. Ras, R.G Wilks, M. Bär, T. Unold, R. Agrawal. "Improved performance of Ge-alloyed CZTGeSSe thin-film solar cells through control of elemental losses". Prog. Photovolt: Res. Appl. 23, (2015), 376–384.

[9] T. Schnabel, M. Seboui and E. Ahlswede, "Evaluation of different metal salt solutions for the preparation of solar cells with wide-gap $Cu_2ZnGeS_xSe_{4-x}$ absorbers" RSC Adv., 7, (2017), 26-30

[10] International Center for Diffraction Data: CZGSe ‐ 00-052-0867; $MoSe_2$ ‐ 04-004-8782; ZnO: 04-015-4060; ZnSe: 04 -015-0312;Mo:01-088-2331.

[11] Alexander P. Litvinchuk, "Optical properties and lattice dynamics of $Cu_2ZnGeSe_4$ quaternary semiconductor: A density-functional study" Phys. Status Solidi B 253, No. 2, (2016),323–328

[12] G. Brammertz, M. Buffi`ere, S. Oueslati, H. El Anzeery, K. BenMessaoud,S. Sahayaraj, C. K¨oble, M. Meuris, and J. Poortmans, "Characterization of defects in 9.7% efficient Cu_2 $ZnSnSe_4$ -CdS-ZnO solar cells," *Appl. Phys.Lett.*, vol. 103, (2013), 163904 1-4,

[13] S. Oueslati, G. Brammertz, M. Buffière, H. ElAnzeery, O.Touayar, C. Köble, J.Bekaert, M. Meuris, J. Poortmans, Physical and Electrical Characterization of High-Performance $Cu_2ZnSnSe_4$ based Thin Film Solar Cells. Thin Solid Films 582, (2015), 224−228.

[14] Scheer, R. & Schock, H. W. Chalcogenide Photovoltaics (2011). Wiley-VCH Verlag Gmbh & Co, KGaA, Weinheim

[15] U. Rau and J. H. Werner, "Radiative efficiency limits of solar cells with lateral band-gap fluctuations", App. Phy. letters, 84, (2004),3735

[16] T. Gershon, B. Shin, N. Bojarczuk, T. Gokmen, S. Lu, and S. Guha, J. Appl. Phys. 114, (2013), 154905

[17] J.I Pankove, Optical Processes in Semiconductors, (1971), Dover, New York.

[18] H.B. Bepp, and E.W. Wiliams, Photoluminescence theory in Semiconductor and Semimetals, (1972) , vol. 8 (eds R.K. Willardson and A.C. Beer) Academic Press, New York.

[19] T. Schmidt, K. Lischka, W. Zulehner, Excitation-power dependence of the near band edge photoluminescence of semiconductors, Phys. Rev. B:Condens.Matter 45,(1992), 8989.

[20] P. W. Yu and Y. S. Park, J. Appl. Phys. 48, (1977), 2434

[21] S. A. Schumacher, J. R. Botha, and V. Alberts, J. Appl. Phys. 99, (2006),063508

[22] F. Luckert, M.V. Yakushev, C. Faugeras, A.V. Karotki, A.V. Mudryi, R.W .Martin, Excitation power and temperature dependence of excitons in $CuInSe_2$, Appl.Phys.Lett.111,(2012), 093507.

[23] U. Rau, D.A. Ras, T. Kirchartz, Photoluminescence analysis of thin-film solar cells, Advanced Characterization Techniques for Thin Film Solar Cells (2011), 151–173.

[24] B.I Shklovskii, and A.L. Efros, Electronic Properties of Doped Semiconductors, (1984) Springer, Berlin.

[25] S. Sahayaraj, G. Brammertz, B. Vermang, S. Ranjbar, M. Meuris , J. Vleugels, J. Poortmans, et al, Effect of the duration of a wet KCN etching step and post deposition annealing on the efficiency of $Cu_2ZnSnSe_4$ solar cells, Thin Solid Films (2016),

[26] A. P. Levanyuk and V. V. Osipov, "Edge luminescence of direct-gap semiconductors,"Sov. Phys. Usp. 24(3), (1981), 187–215

[27] T. Gokmen, O.Gunawan, T.K. Todorov, D.B. Mitzi "Band tailing and efficiency limitation in kesterite solar cells" App. Phy. Lett. 103, (2013), 103506